Available online at www.sciencedirect.com
SCIENCE DIRECT®
Comput. Methods Appl. Mech. Engrg. 192 (2003) 3909–3932
Computer methods in applied mechanics and engineering
www.elsevier.com/locate/cma

Topology optimization of flow networks

Anders Klarbring [a,*], Joakim Petersson [a,1], Bo Torstenfelt [a], Matts Karlsson [b]

[a] Department of Mechanical Engineering, Linköping University, SE-581 83 Linköping, Sweden
[b] Department of Biomedical Engineering and National Supercomputer Centre, Linköping University, SE-581 83 Linköping, Sweden

Received 9 October 2002; received in revised form 6 May 2003; accepted 8 May 2003

Abstract

The field of topology optimization is well developed for load carrying trusses, but so far not for other similar network problems. The present paper is a first study in the direction of topology optimization of flow networks. A linear network flow model based on Hagen–Poiseuille's equation is used. Cross-section areas of pipes are design variables and the objective of the optimization is to minimize a measure, which in special cases represents dissipation or pressure drop, subject to a constraint on the available (generalized) volume. A ground structure approach where cross-section areas may approach zero is used, whereby the optimal topology (and size) of the network is found.

A substantial set of examples is presented: small examples are used to illustrate difficulties related to non-convexity of the optimization problem; larger arterial tree-type networks, with bio-mechanics interpretations, illustrate basic properties of optimal networks; the effect of volume forces is exemplified.

We derive optimality conditions which turns out to contain Murray's law; thereby, presenting a new derivation of this well known physiological law. Both our numerical algorithm and the derivation of optimality conditions are based on an ε-perturbation where cross-section areas may become small but stay finite. An indication of the correctness of this approach is given by a theorem, the proof of which is presented in an appendix.

1. Introduction

Linear network problems arise in several areas of engineering science (see, for instance [21]): in structural mechanics the truss problem consists in the finding of stresses and displacements in a network of bars; in fluid mechanics (or hydraulics) one wants to find pressures and flows in a network of pipes; and in electrical engineering there is the problem of finding voltage and currents in an electrical network. In structural mechanics much effort has been put into finding methods for optimizing a load carrying truss. In particular, there is a body of theory and computational algorithms that deals with obtaining an optimal topology, or connectivity, of a truss (see the review paper [6]). Here the topology of a truss is obtained by the so-called ground structure approach in which a very large number of potential bars are given at the outset.

* Corresponding author. Tel.: +46-13-281-117; fax: +46-13-281-101.
E-mail addresses: andkl@ikp.liu.se (A. Klarbring), botor@ikp.liu.se (B. Torstenfelt), matka@imt.liu.se (M. Karlsson).
[1] Deceased on September 30, 2002.

0045-7825/$ - see front matter © 2003 Elsevier B.V. All rights reserved.
doi:10.1016/S0045-7825(03)00393-1

Cross-section areas of these bars are then chosen as design variables in the optimization process and are allowed to take the value zero (or close to zero). In this way the topology (and size) of the most preferable truss is chosen. Surprisingly enough the theory and techniques of truss topology optimization do not seem to have been transferred to any of the other network problems mentioned above.

It is the purpose of this paper to extend and apply procedures from truss topology optimization to fluid mechanics, or simply, flow networks. A linear model representing such networks is derived on an assumption of laminar flow in each pipe, leading to Hagen–Poiseuille's equation, replacing Hooke's law of linear elasticity in the case of a truss (or Ohm's law in electrical networks). Design variables are chosen to be cross-section areas of pipes. Since these areas may approach zero, a ground structure strategy is used where pipes are removed and an optimal topology is found. As an objective function we use the potential function of the state problem, which in special cases implies minimizing dissipation or maximizing flow.

An initial influence for this work was a series of papers by Schreiner and co-workers [15–17]. In these papers the goal is to generate, by computational means, arterial or vascular trees and investigate if general optimization principles can explain the overall structure of such trees. However, the approach generates trees in a step-wise fashion, without ever stating an overall optimization problem and, therefore, our impression is that it is hard to say if it is an optimization principle or the algorithm which is responsible for a particular outcome. The approach used here is largely freed from any influence of the algorithmic treatment: a clear overall optimization problem is stated, which can be solved by a number of suitable algorithms. Arterial tree-like structures are treated in Section 6.2. Another work which also has been an inspiration for the present study is the book by Bejan [4].

Network flow problems is an extensive area within operations research [2]. However, the networks considered there are different from the ones under consideration in this paper. Our problem is based on a linear state problem which, at least for the case of non-zero areas, has a unique solution. This linear state problem is based on Kirchhoff's law at the nodes and a linear constitutive law (Hagen–Poiseuille's equation, Hooke's law or Ohm's law). The problems considered within operations research are based on Kirchhoff's law and maximum arc capacities. For someone with a background in structural mechanics it may be useful to understand this difference as analogous to the difference between elastic analysis and plastic limit state analysis. These facts are elegantly explained by Prager [18] and can also be appreciated from Dennis [9]. Another problem with at least a superficial resemblance with the problem considered in this paper is the problem of optimal water distribution networks [7].

Following this introduction we derive in Section 2 the state problem of flow in networks and prove some of its basic properties such as uniqueness of solutions. In Section 3 the optimization problem is stated, and its meaning and basic properties are discussed. Section 4 contains a derivation of optimality conditions, based on an ε-perturbation of the problem. A theorem which indicates convergence of the solution to the original problem as ε goes to zero is stated and proved in Appendix A. In Section 5 a numerical algorithm for solution of the optimization problem is presented. In Section 6 numerical examples are solved to illustrate properties of optimal solutions. Finally, in Section 7, we give some suggestions for further work.

2. State problem

2.1. Basic equations

Consider a network consisting of n nodes or junctions and m segments or pipes (see Fig. 1). The fluid flow within each segment is assumed to be governed by an extension [2] of Hagen–Poiseuille's equation, which is

[2] The extension being that volume force is included.

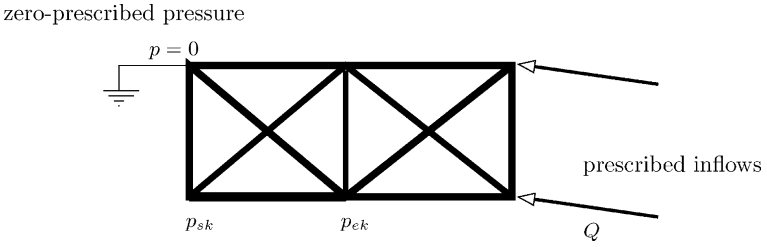

Fig. 1. A small flow network.

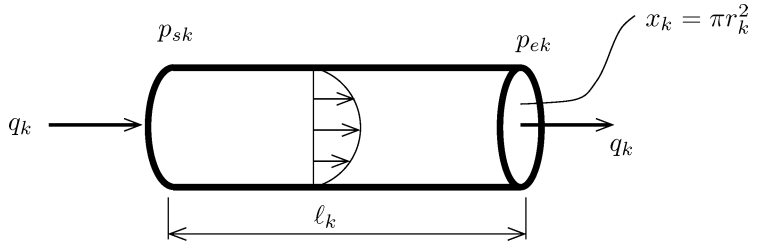

Fig. 2. A pipe in which the flow follows the Hagen–Poiseuille equation.

derived from Navier–Stokes' equations under the assumptions that the cross-section of a pipe is circular and that the velocity has a component only in the pipe direction, the latter meaning laminar flow (cf. Fig. 2). Let p_{sk} and p_{ek} be the pressures at the start and end nodes of segment k, respectively; furthermore, q_k, x_k and ℓ_k are volume flow, cross-section area and length of segment k, while f_k represents a constant force per volume in the direction of the segment. [3] Then, the extended Hagen–Poiseuille equation reads

$$q_k = \frac{x_k^2}{8\pi\mu\ell_k}(p_{sk} - p_{ek} + f_k\ell_k), \tag{1}$$

where μ is the viscosity of the fluid which is a constant.

The start and end pressures of segments are connected by the fact that there is one unique pressure at each node. Let the pressures at nodes be collected in an n-vector $\boldsymbol{p} = (p_1, \ldots, p_n)^\top$, where $\top$ indicates transpose of a vector or matrix. Then, for each segment, $k = 1, \ldots, m$,

$$p_{sk} - p_{ek} = \boldsymbol{\gamma}_k^\top \boldsymbol{p}, \tag{2}$$

where $\boldsymbol{\gamma}_k$ is an n-vector with numbers 1 and -1 in two positions, corresponding to the connected nodes, and 0 in all other positions.

Since we are treating an incompressible fluid, the volume flow provided to a node through connecting segments add up to the volume flow leaving the network at the node (Kirchhoff's law). By the structure of the $\boldsymbol{\gamma}_k$'s one conclude that such balance of flow at each node results in the equation

$$\sum_{k=1}^{m} \boldsymbol{\gamma}_k q_k = \boldsymbol{Q}, \tag{3}$$

where $\boldsymbol{Q}$ is a vector of external inflows, Q_k, to the network at the nodes.

[3] The assumption of a constant force within each segment is not essential, but made for convenience of presentation.

Eqs. (1)–(3) give

$$\sum_{k=1}^{m} \gamma_k \left[\frac{x_k^2}{8\pi\mu\ell_k} (\gamma_k^\top \boldsymbol{p} + f_k \ell_k) \right] = \boldsymbol{Q}. \tag{4}$$

In full matrix form this reads

$$\boldsymbol{B}^\top \boldsymbol{D}(\boldsymbol{x})(\boldsymbol{B}\boldsymbol{p} + \boldsymbol{f}) = \boldsymbol{Q}, \tag{5}$$

where $\boldsymbol{B}$ is an m by n matrix where $\gamma_k^\top$'s make up the rows, $\boldsymbol{f}$ is a force vector of length m whose elements are $f_k \ell_k$ and $\boldsymbol{D}(\boldsymbol{x})$ is the m by m diagonal matrix

$$\boldsymbol{D}(\boldsymbol{x}) = \text{diag } \{D_k(x_k)\}, \quad D_k(x_k) = \frac{x_k^2}{8\pi\mu\ell_k}.$$

This matrix is taken to depend on the m-vector $\boldsymbol{x} = (x_1, \ldots, x_m)^\top$ of cross-section areas. The reason being that this vector will act as design variable in the optimization problem to be formulated below. Note that $\boldsymbol{x} \geqslant \boldsymbol{0}$ and that it is essential for the idea of topology optimization that we allow individual areas to become zero: it is when this happens that pipes are removed from the so-called ground structure and different topologies of the remaining network are possible.

Remark 1. It may be useful for ones understanding of the structure of (5) to note that, when $\boldsymbol{x} > \boldsymbol{0}$, so that $\boldsymbol{D}(\boldsymbol{x})$ is non-singular, it can be written in the following form:

$$\boldsymbol{D}(\boldsymbol{x})^{-1} \boldsymbol{q} - \boldsymbol{B}\boldsymbol{p} = \boldsymbol{f}, \tag{6}$$

$$\boldsymbol{B}^\top \boldsymbol{q} = \boldsymbol{Q}, \tag{7}$$

where $\boldsymbol{q}$ is an m-vector of volume flows. Note that these equations have the same structure as those of a truss where nodes are connected by linear elastic bars. The analogy follows by the following changes of interpretations: displacement $\leftrightarrow$ pressure ($\boldsymbol{p}$), stress $\leftrightarrow$ volume flow ($\boldsymbol{q}$), force $\leftrightarrow$ inflow ($\boldsymbol{Q}$) and initial strain $\leftrightarrow$ force ($\boldsymbol{f}$). There is, however, one main difference between the equations of flow networks and those of an elastic truss: the analogy of the matrix $\boldsymbol{D}(\boldsymbol{x})$ of a truss depends linearly on areas, whereas the dependence is quadratic for flow networks. A consequence of this, to be seen below, is that the resulting topology optimization problem becomes non-convex for flow networks while it is convex for trusses.

When some elements of $\boldsymbol{x}$ are allowed to take the value zero, Eq. (6) is not valid. However we may still write

$$\boldsymbol{q} = \boldsymbol{D}(\boldsymbol{x})(\boldsymbol{B}\boldsymbol{p} + \boldsymbol{f}),$$

which is simply the matrix form of Eq. (1). We conclude that when $x_k = 0$ for some k the corresponding q_k also becomes zero, while pressures may become undetermined.

Remark 2. The dissipation in a fluid can generally be written as the volume integral over the inner product between stress and rate-of-deformation tensors. The assumptions underlying Hagen–Poiseuille flow result in that this dissipation can be written as

$$d = \sum_k \frac{q_k^2}{D_k(x_k)} = (\boldsymbol{B}\boldsymbol{p} + \boldsymbol{f})^\top \boldsymbol{D}(\boldsymbol{x})(\boldsymbol{B}\boldsymbol{p} + \boldsymbol{f}),$$

where $\sum_k$ denotes the sum over all indices k for which $x_k > 0$.

2.2. Properties of basic equations

In the following we will need the concept of a connected network: a network is *connected* if any node can be reached from any other node by following segments.

Proposition 1. *If the network is connected then*

$$\boldsymbol{B}\boldsymbol{p} = \boldsymbol{0} \Longleftrightarrow p_1 = p_2 = \cdots = p_n.$$

Proof. The left hand implication ($\Leftarrow$) is obvious from the structure of $\boldsymbol{B}$.

The left hand equation in the above equivalence can be written as $\gamma_k \boldsymbol{p} = 0$, $k = 1, \ldots, m$. Now, $\gamma_k \boldsymbol{p} = 0$ implies $p_k = p_j$ for nodes i and j connected by segment k. Since any node is connected to some other node by at least one segment, the right hand implication ($\Rightarrow$) follows. □

Introduce the notation $\boldsymbol{K}(\boldsymbol{x}) = \boldsymbol{B}^\top \boldsymbol{D}(\boldsymbol{x})\boldsymbol{B}$ for the system matrix of the linear system (5).

Proposition 2. *The system matrix $\boldsymbol{K}(\boldsymbol{x})$ is positive semi-definite.*

Proof. Let $\boldsymbol{y} = \boldsymbol{B}\boldsymbol{p}$ for some $\boldsymbol{p}$. Then $\boldsymbol{p}^\top \boldsymbol{K}(\boldsymbol{x})\boldsymbol{p} = \boldsymbol{y}^\top \boldsymbol{D}(\boldsymbol{x})\boldsymbol{y}$, which is greater than or equal to zero since $\boldsymbol{D}(\boldsymbol{x})$ is positive semi-definite. □

Note that this proposition holds even when $x_k = 0$ for some k and/or the network is not connected.

Proposition 3. *If the network is connected and $\boldsymbol{x} > \boldsymbol{0}$, then the null spaces of $\boldsymbol{K}(\boldsymbol{x})$ and $\boldsymbol{B}$ are equal, i.e.,*

$$\boldsymbol{K}(\boldsymbol{x})\boldsymbol{p} = \boldsymbol{0} \Longleftrightarrow \boldsymbol{B}\boldsymbol{p} = \boldsymbol{0} \Longleftrightarrow p_1 = p_2 = \cdots = p_n,$$

where the second equivalence was stated already in Proposition 1.

Proof. The left hand implication ($\Leftarrow$) is obvious from the structure of $\boldsymbol{K}(\boldsymbol{x})$. The right hand implication follows from

$$\boldsymbol{K}(\boldsymbol{x})\boldsymbol{p} = \boldsymbol{0} \Rightarrow \boldsymbol{p}^\top \boldsymbol{K}(\boldsymbol{x})\boldsymbol{p} = (\boldsymbol{B}\boldsymbol{p})^\top \boldsymbol{D}(\boldsymbol{x})(\boldsymbol{B}\boldsymbol{p}) = 0 \Rightarrow \boldsymbol{B}\boldsymbol{p} = \boldsymbol{0},$$

where the last implication follows from the fact that $\boldsymbol{D}(\boldsymbol{x})$ is positive definite when $\boldsymbol{x} > \boldsymbol{0}$ and the network is connected. □

Proposition 4. *Let $\boldsymbol{x} > \boldsymbol{0}$ and let the network be connected. Then a necessary and sufficient condition for the existence of a pressure $\boldsymbol{p}$ that satisfies* (5) *is that*

$$\sum_{i=1}^{n} Q_k = \boldsymbol{1}^\top \boldsymbol{Q} = 0, \tag{8}$$

where $\boldsymbol{1}$ is an n-vector of ones. If $x_k = 0$ for some k and/or the network is not connected, then this condition is necessary for the existence of a pressure but in general not sufficient.

Proof. A standard result of linear algebra is that a necessary and sufficient condition for the solvability of a linear system $Ax = f$, where A is a square matrix and x and f vectors, x being the solution vector, is that f is orthogonal to the null space of A. Applying this to (5), and using Proposition 3, one finds that $\boldsymbol{Q} - \boldsymbol{B}^\top \boldsymbol{D}(\boldsymbol{x})\boldsymbol{f}$ should be orthogonal to $\boldsymbol{1}$. Since, from Proposition 1, $\boldsymbol{B}\boldsymbol{1} = \boldsymbol{0}$ the first result follows.

The second result follows from the fact that the null space of $\boldsymbol{K}(\boldsymbol{x})$ may be enlarged when $x_k = 0$ for some k or when the network is not connected, but it may not become smaller. □

Remark 3. Eq. (8) has the interpretation that there will always be a balance between inflow and outflow of fluid.

2.3. Boundary conditions and state problem

The equation that connects pressure and inflow at nodes is given by (5) (or equivalently by (4)). A well-posed problem may be obtained from this equation by, at each node, specifying pressure or volume flow as known, assuming that the vector of forces $\boldsymbol{f}$ is also a known quantity. The set of nodes $\{1,\ldots,n\}$ is decomposed into disjoint subsets α and β such that $\alpha \cup \beta = \{1,\ldots,n\}$. For nodes belonging to α the volume flow is known, i.e.,

$$Q_i = \overline{Q}_i, \quad i \in \alpha \Longleftrightarrow \boldsymbol{Q}_\alpha = \overline{\boldsymbol{Q}}_\alpha \tag{9}$$

and for nodes belonging to β the pressure is known, i.e.,

$$p_i = \bar{p}_i, \quad i \in \beta \Longleftrightarrow \boldsymbol{p}_\beta = \bar{\boldsymbol{p}}_\beta, \tag{10}$$

where a bar indicates known quantities and we have used the notation $\boldsymbol{y}_\alpha$ for a subvector of $\boldsymbol{y}$ that contains elements with indices in α. In the following we will also use the notation $\boldsymbol{A}_{\alpha\beta}$ for a submatrix of matrix $\boldsymbol{A}$ consisting of rows belonging to α and columns belonging to β.

The *state problem* is now to solve Eqs. (5), (9) and (10) for $\boldsymbol{p}$ and $\boldsymbol{Q}$, or, equivalently, for $\boldsymbol{p}_\alpha$ and $\boldsymbol{Q}_\beta$.

Proposition 5. *Assume that β contains at least one index (= node), $\boldsymbol{x} > \boldsymbol{0}$ and that the network is connected. Then the state problem has a unique solution.*

Proof. Using (9) and (10) in (5) the state problem takes the following form:

$$\boldsymbol{K}_{\alpha\alpha}(\boldsymbol{x})\boldsymbol{p}_\alpha + \boldsymbol{K}_{\alpha\beta}(\boldsymbol{x})\bar{\boldsymbol{p}}_\beta = \bar{\boldsymbol{Q}}_\alpha - \boldsymbol{B}_\alpha^\top \boldsymbol{D}(\boldsymbol{x})\boldsymbol{f}, \tag{11}$$

$$\boldsymbol{K}_{\beta\alpha}(\boldsymbol{x})\boldsymbol{p}_\alpha + \boldsymbol{K}_{\beta\beta}(\boldsymbol{x})\bar{\boldsymbol{p}}_\beta = \boldsymbol{Q}_\beta - \boldsymbol{B}_\beta^\top \boldsymbol{D}(\boldsymbol{x})\boldsymbol{f}. \tag{12}$$

Note that we may write

$$\boldsymbol{K}_{\alpha\beta}(\boldsymbol{x}) = \boldsymbol{B}_\alpha^\top \boldsymbol{D}(\boldsymbol{x})\boldsymbol{B}_\beta,$$

where $\boldsymbol{B}_\alpha$ indicates the submatrix of $\boldsymbol{B}$ consisting of columns with indices in α.

We now show that $\boldsymbol{K}_{\alpha\alpha}(\boldsymbol{x})$ is positive definite ($\Rightarrow$ non-singular). That it is positive semi-definite follows from Proposition 2. Next we conclude that

$$\boldsymbol{p}_\alpha^\top \boldsymbol{K}_{\alpha\alpha}(\boldsymbol{x})\boldsymbol{p}_\alpha = 0 \Rightarrow \boldsymbol{p}_\alpha = \boldsymbol{0}.$$

This follows from Proposition 3 and

$$\boldsymbol{p}_\alpha^\top \boldsymbol{K}_{\alpha\alpha}(\boldsymbol{x})\boldsymbol{p}_\alpha = \begin{bmatrix} \boldsymbol{p}_\alpha^\top & \boldsymbol{0}^\top \end{bmatrix} \boldsymbol{K}(\boldsymbol{x}) \begin{bmatrix} \boldsymbol{p}_\alpha \\ \boldsymbol{0} \end{bmatrix},$$

where, without loss of generality, we have assumed a particular ordering of indices. Thus, $\boldsymbol{p}_\alpha$ may be uniquely solved from (11) and when substituting this into (12) one obtains $\boldsymbol{Q}_\beta$. □

3. Optimization problem

In this section we formulate the optimization problem. As indicated in the introduction, we chose a strategy which is inspired by the ground structure approach in truss topology optimization. That is, a ground structure, consisting of a very large number of members, in this case pipes, are constructed. Then cross-section areas of pipes are taken as design variables and are allowed to take the value zero (or close to zero, see below). In this way pipes may be removed from the ground structure and remaining pipes form a network which is a competitor in the optimization process. Note that when cross-section areas go to zero, the flow in the pipe also vanishes while pressures may become undetermined.

Let $\boldsymbol{p}(\boldsymbol{x})$ and $\boldsymbol{Q}(\boldsymbol{x})$ denote any solution $\boldsymbol{p}$ and $\boldsymbol{Q}$ of the state problem

$$\boldsymbol{B}^{\top}\boldsymbol{D}(\boldsymbol{x})(\boldsymbol{B}\boldsymbol{p}+\boldsymbol{f})=\boldsymbol{Q},\quad \boldsymbol{Q}_{\alpha}=\overline{\boldsymbol{Q}}_{\alpha},\quad \boldsymbol{p}_{\beta}=\bar{\boldsymbol{p}}_{\beta}. \tag{13}$$

Alternatively, for obvious reasons, we also consider subvectors $\boldsymbol{p}_{\alpha}(\boldsymbol{x})$ and $\boldsymbol{Q}_{\beta}(\boldsymbol{x})$ of $\boldsymbol{p}(\boldsymbol{x})$ and $\boldsymbol{Q}(\boldsymbol{x})$ as a solution of (13).

Since $\boldsymbol{B}^{\top}\boldsymbol{D}(\boldsymbol{x})\boldsymbol{B}$ is positive semi-definite, problem (13) can equivalently be stated as a minimization problem. Introduce the set of feasible pressures

$$\mathscr{P}=\{\boldsymbol{p}\mid \boldsymbol{p}_{\beta}=\bar{\boldsymbol{p}}_{\beta}\}$$

and the potential

$$\Pi(\boldsymbol{p},\boldsymbol{x})=\tfrac{1}{2}(\boldsymbol{B}\boldsymbol{p}+\boldsymbol{f})^{\top}\boldsymbol{D}(\boldsymbol{x})(\boldsymbol{B}\boldsymbol{p}+\boldsymbol{f})-\overline{\boldsymbol{Q}}_{\alpha}^{\top}\boldsymbol{p}_{\alpha}.$$

Then, $\boldsymbol{p}(\boldsymbol{x})$ is a solution of

$$\Pi(\boldsymbol{p},\boldsymbol{x})=\inf_{\boldsymbol{p}^{*}\in\mathscr{P}}\Pi(\boldsymbol{p}^{*},\boldsymbol{x}). \tag{14}$$

Furthermore, $\boldsymbol{Q}_{\beta}(\boldsymbol{x})$ is a Lagrangian multiplier vector of the constraint $\boldsymbol{p}^{*}\in\mathscr{P}$. Note also that when $\overline{\boldsymbol{Q}}_{\alpha}$ equals zero, (14) means minimizing dissipation.

From the theory of quadratic programming we conclude that when $\boldsymbol{B}^{\top}\boldsymbol{D}(\boldsymbol{x})\boldsymbol{B}$ is singular, (14), and thus also (13), may lack a solution or have several solutions. When there is no solution the infimum in (14) becomes unbounded and when there are several solutions they all give the same value $\Pi(\boldsymbol{p}(\boldsymbol{x}),\boldsymbol{x})$.

As a design goal we attempt to find a design $\boldsymbol{x}$ satisfying some size restrictions to be stated below and such that

$$-\varphi(\boldsymbol{x})=\inf_{\boldsymbol{p}^{*}\in\mathscr{P}}\Pi(\boldsymbol{p}^{*},\boldsymbol{x}) \tag{15}$$

becomes as large as possible, or, alternatively, $\varphi(\boldsymbol{x})$ is minimized. This design objective has a number of important properties. Firstly, we note that designs $\boldsymbol{x}$ such that (13) has no solution are not competitive in the optimization process since $\varphi(\boldsymbol{x})$ then takes the value $+\infty$. Furthermore, designs for which there are several solutions are, nevertheless, such that $\varphi(\boldsymbol{x})$ has a unique value.

As what concerns the physical interpretation of $\varphi(\boldsymbol{x})$ we study this for a design $\boldsymbol{x}$ for which $\varphi(\boldsymbol{x})$ is finite, i.e., it holds that

$$\varphi(\boldsymbol{x})=\overline{\boldsymbol{Q}}_{\alpha}^{\top}\boldsymbol{p}_{\alpha}(\boldsymbol{x})-\tfrac{1}{2}(\boldsymbol{B}\boldsymbol{p}(\boldsymbol{x})+\boldsymbol{f})^{\top}\boldsymbol{D}(\boldsymbol{x})(\boldsymbol{B}\boldsymbol{p}(\boldsymbol{x})+\boldsymbol{f}). \tag{16}$$

By using (13) one finds

$$\varphi(\boldsymbol{x})=\tfrac{1}{2}\overline{\boldsymbol{Q}}_{\alpha}^{\top}\boldsymbol{p}_{\alpha}(\boldsymbol{x})-\tfrac{1}{2}\bar{\boldsymbol{p}}_{\beta}^{\top}\boldsymbol{Q}_{\beta}(\boldsymbol{x})-\tfrac{1}{2}\boldsymbol{f}^{\top}\boldsymbol{q}(\boldsymbol{x}), \tag{17}$$

where $\boldsymbol{q}(\boldsymbol{x})=\boldsymbol{D}(\boldsymbol{x})(\boldsymbol{B}\boldsymbol{p}(\boldsymbol{x})+\boldsymbol{f})$ is the volume flow. To get a feel for (17) we study some special cases:

(1) Let the volume force be zero, i.e, $\boldsymbol{f} = \mathbf{0}$, and take the prescribed pressure to be uniform, i.e,

$$\bar{\boldsymbol{p}}_\beta = \mathbf{1}_\beta p_{\text{fix}},$$

where $\mathbf{1}$ is a vector of ones and p_{fix} is the prescribed pressure. We may use the solvability condition (8) to rewrite $\varphi(\boldsymbol{x})$. This condition may be written $\mathbf{1}_\beta^\top \boldsymbol{Q}_\beta(\boldsymbol{x}) = -\mathbf{1}_\alpha^\top \overline{\boldsymbol{Q}}_\alpha$. Using this and the condition of uniform pressure, (17) results in

$$\varphi(\boldsymbol{x}) = \tfrac{1}{2}\overline{\boldsymbol{Q}}_\alpha^\top \boldsymbol{p}_\alpha(\boldsymbol{x}) + \tfrac{1}{2}\mathbf{1}_\alpha^\top \overline{\boldsymbol{Q}}_\alpha p_{\text{fix}}, \tag{18}$$

where the second term is a prescribed constant and thus has no influence on the optimization problem. Thus, our design goal is to minimize those pressures where inflow is prescribed and maximize those where outflow is prescribed: the "pressure loss" is to be minimized. Moreover, since the dissipation can be written as

$$d(\boldsymbol{x}) = \overline{\boldsymbol{Q}}_\alpha^\top \boldsymbol{p}_\alpha(\boldsymbol{x}) + \bar{\boldsymbol{p}}_\beta \boldsymbol{Q}_\beta(\boldsymbol{x}) = \overline{\boldsymbol{Q}}_\alpha^\top \boldsymbol{p}_\alpha(\boldsymbol{x}) - \mathbf{1}_\alpha^\top \overline{\boldsymbol{Q}}_\alpha p_{\text{fix}} \tag{19}$$

by using (11) and (12), the objective can also be written

$$\varphi(\boldsymbol{x}) = \frac{d(\boldsymbol{x})}{2} + \mathbf{1}_\alpha^\top \overline{\boldsymbol{Q}}_\alpha p_{\text{fix}}, \tag{20}$$

which means that we are minimizing the dissipation.

(2) As further specialization of the above item we may take $\overline{\boldsymbol{Q}}_\alpha$ to represent a uniform outflow, i.e.

$$\overline{\boldsymbol{Q}}_\alpha = -Q_{\text{out}}\mathbf{1}_\alpha, \quad Q_{\text{out}} > 0.$$

Then, (19) becomes

$$d(\boldsymbol{x}) = Q_{\text{out}} n_\alpha \left(p_{\text{fix}} - \frac{\mathbf{1}_\alpha^\top \boldsymbol{p}_\alpha(\boldsymbol{x})}{n_\alpha} \right), \tag{21}$$

where n_α is the number of elements in α. The term $\mathbf{1}_\alpha^\top \boldsymbol{p}_\alpha(\boldsymbol{x})/n_\alpha$ is the average pressure at outflow nodes. Since the dissipation is greater than zero, p_{fix} is greater than this value and p_{fix} represents an inflow pressure, hence the design goal is to minimize the difference between the inflow pressure and the average outflow pressure.

(3) Let the prescribed flow be zero, i.e., $\overline{\boldsymbol{Q}}_\alpha = \mathbf{0}$, so

$$\varphi(\boldsymbol{x}) = -\tfrac{1}{2}\bar{\boldsymbol{p}}_\beta^\top \boldsymbol{Q}_\beta(\boldsymbol{x}) - \tfrac{1}{2}\boldsymbol{f}^\top \boldsymbol{q}(\boldsymbol{x}). \tag{22}$$

Thus, the design goal is to maximize flow when weighted by $\bar{\boldsymbol{p}}_\beta$ and $\boldsymbol{f}$.

We now state our optimization problem as

$$(\mathscr{P})_0 \begin{cases} \min\limits_{\boldsymbol{x}} & \varphi(\boldsymbol{x}), \\ \text{subject to} & v(\boldsymbol{x}) \leqslant V, \quad \bar{\boldsymbol{x}} \geqslant \boldsymbol{x} \geqslant \mathbf{0}, \end{cases}$$

where $\bar{\boldsymbol{x}}$ is an upper bound on the cross-section areas,

$$v(\boldsymbol{x}) = \sum_{k=1}^{m} x_k^\sigma \ell_k$$

and $\sigma > 0$ and $V > 0$ are a constants. For $\sigma = 1$, $v(\boldsymbol{x})$ represents the volume of the structure and V is obviously a maximum volume. When $\sigma \neq 1$ we talk of optimization under a "generalized volume" constraint. The reason for introducing a generalization of a volume constraint will be apparent when we derive optimality conditions in Section 4: these conditions will relate to a generalization of Murray's law, used, for instance, by Schreiner et al. [16].

Problem $(\mathscr{P})_0$ involves two functionals: $\varphi(\boldsymbol{x})$, which for the case of a uniform prescribed pressure can be seen as the dissipation, and $v(\boldsymbol{x})$, which represents (generalized) volume. In words our problem is therefore to minimize dissipation under a volume constraint. A natural question is whether this problem is related to the "reversed" problem of minimizing volume under a constraint on dissipation. For the special case when the upper bound on $\boldsymbol{x}$, i.e., $\bar{\boldsymbol{x}}$, is removed from the problem, $\bar{\boldsymbol{p}}_\beta$ is uniform and $\boldsymbol{f} = \boldsymbol{0}$, this question has an exact answer: we may obtain the solution of either of the two problems from the solution of the other by appropriate scaling. Furthermore, we may define a third problem which is to minimize the sum of dissipation and a constant times volume and the solution of this problem follows from a scaling of a solution to one of the first two problems. This later fact is of interest since such a problem in terms of a sum of dissipation and volume has been been extensively studied in a bio-mechanical context (see [22]). Proofs of the above claims will be published in a forthcoming paper and are based on theory that can be found in [19].

Another important result, which can also be established following [19], is that, for the special case of $\bar{\boldsymbol{x}}$ removed, $\bar{\boldsymbol{p}}_\beta$ uniform, and $\boldsymbol{f} = \boldsymbol{0}$, solutions of $(\mathscr{P})_0$ are *self-similar*. To be more precise, let $\boldsymbol{x}_0^1$ be a solution of $(\mathscr{P})_0$ with $V = 1$, then a solution for a general V, denoted $\boldsymbol{x}_0$, follows as $\boldsymbol{x}_0 = V^{1/\sigma}\boldsymbol{x}_0^1$.

4. ε-Perturbation and optimality conditions

One difficulty associated with problem $(\mathscr{P})_0$ is the possible non-solvability of the state problem that may occur when some cross-section areas become zero. A strategy to avoid this problem, frequently used in analogous problems in structural optimization, is to introduce an ε-perturbation of $(\mathscr{P})_0$, i.e., let $\varepsilon > 0$ and define the following optimization problem:

$$(\mathscr{P})_\varepsilon \begin{cases} \min\limits_{\boldsymbol{x}} & \varphi(\boldsymbol{x}), \\ \text{subject to} & v(\boldsymbol{x}) \leqslant V, \quad \bar{\boldsymbol{x}} \geqslant \boldsymbol{x} \geqslant \varepsilon \boldsymbol{1}. \end{cases}$$

From now on, we assume that the network is connected and $\beta \neq \emptyset$. Then, by Proposition 5, for any $\boldsymbol{x}$ belonging to the feasible set of this problem, the state problem is uniquely solvable and $\varphi(\boldsymbol{x})$ is finite. The function φ can be written as pointwise maxima of an indexed family of functions, i.e.

$$\varphi(\boldsymbol{x}) = \max_{\boldsymbol{p} \in \mathscr{P}} \left(\overline{\boldsymbol{Q}}_\alpha^\top \boldsymbol{p}_\alpha - \tfrac{1}{2}(\boldsymbol{B}\boldsymbol{p} + \boldsymbol{f})^\top \boldsymbol{D}(\boldsymbol{x})(\boldsymbol{B}\boldsymbol{p} + \boldsymbol{f}) \right)$$

and so we can apply theorems on generalized gradients for such functions. In fact, it follows from Theorem 2.8.6 in [8] that

$$\frac{\partial \varphi(\boldsymbol{x})}{\partial x_k} = -\frac{1}{2}(\boldsymbol{B}\boldsymbol{p}(\boldsymbol{x}) + \boldsymbol{f})^\top \frac{\partial \boldsymbol{D}(\boldsymbol{x})}{\partial x_k}(\boldsymbol{B}\boldsymbol{p}(\boldsymbol{x}) + \boldsymbol{f}) \tag{23}$$

since now the minimizing vector $\boldsymbol{p}(\boldsymbol{x})$ always exists uniquely. This expression for the derivative of the objective function will be used in the solution algorithm to be presented in Section 5 and in this section to derive optimality conditions for $(\mathscr{P})_\varepsilon$. However, first we present a proposition to the effect that the ε-perturbation is a valid regularization of $(\mathscr{P})_0$.

Certainly, as we have perturbed the original problem $(\mathscr{P})_0$, we need to know if the optimal solutions of $(\mathscr{P})_\varepsilon$ have anything to do with those of $(\mathscr{P})_0$. Let $\Omega^*(\varepsilon)$ be the set of all globally optimal solutions to $(\mathscr{P})_\varepsilon$, $\varepsilon \geqslant 0$. The question is if $\Omega^*(\varepsilon)$ depends continuously on ε at $\varepsilon = 0$. This is in a sense not intuitively clear since there is a fundamental difference between feasible designs of $(\mathscr{P})_\varepsilon$ and $(\mathscr{P})_0$—the former can represent only one single topology. However, we can prove the following:

Proposition 6. *Suppose* $\{\boldsymbol{x}^*(\varepsilon)\}$ *is any sequence of globally optimal solutions to* $(\mathscr{P})_\varepsilon$ *as* $\varepsilon \to 0$. *Then there exists a convergent subsequence, and for any such subsequential limit* $\boldsymbol{x}^*$, *it holds that* $\boldsymbol{x}^*$ *is a globally optimal solution to* $(\mathscr{P})_0$. *In other words, using a terminology from set-valued analysis* [1], *the solution set map* $\varepsilon \mapsto \Omega^*(\varepsilon)$ *is upper semi-continuous at* $\varepsilon = 0$,

$$\limsup_{\varepsilon\to 0}\Omega^*(\varepsilon)\subset\Omega^*(0),$$

i.e. the upper set limit of $\Omega^*(\varepsilon)$ *is a subset of* $\Omega^*(0)$ *as* $\varepsilon\to 0$.

Proof. Quite technical and therefore postponed to Appendix A. □

This proposition means that if one has succeeded in finding a global optimum of $(\mathscr{P})_\varepsilon$, then this design will be close to some solution of $(\mathscr{P})_0$ if only ε is small enough. [4]

In order to be able to write optimality conditions for $(\mathscr{P})_\varepsilon$ we assume that the data are such that

$$\bar{\boldsymbol{x}}>\varepsilon\mathbf{1},\quad \varepsilon^\sigma\sum_{k=1}^m\ell_k<V.$$

Then the Slater constraint qualification [3], is satisfied and the Karush–Kuhn–Tucker (KKT) conditions become necessary for optimality of $(\mathscr{P})_\varepsilon$. These conditions are

$$-\frac{\partial\varphi(\boldsymbol{x})}{\partial x_k}=\lambda_V\frac{\partial v(\boldsymbol{x})}{\partial x_k}+\lambda_{uk}-\lambda_{lk},\quad k=1,\dots,m, \tag{24}$$

$$\lambda_V\geqslant 0,\quad v(\boldsymbol{x})\leqslant V,\quad \lambda_V(v(\boldsymbol{x})-V)=0, \tag{25}$$

$$\boldsymbol{\lambda}_u\geqslant\mathbf{0},\quad \bar{\boldsymbol{x}}\geqslant\boldsymbol{x},\quad \boldsymbol{\lambda}_u^\top(\bar{\boldsymbol{x}}-\boldsymbol{x})=0, \tag{26}$$

$$\boldsymbol{\lambda}_l\geqslant\mathbf{0},\quad \boldsymbol{x}\geqslant\varepsilon\mathbf{1},\quad \boldsymbol{\lambda}_l^\top(\boldsymbol{x}-\varepsilon\mathbf{1})=0, \tag{27}$$

where the m-vectors $\boldsymbol{\lambda}_u$ and $\boldsymbol{\lambda}_l$ have components λ_{uk} and λ_{lk}, respectively.

For the interpretation of (24) we study an index k such that $\bar{x}_k>x_k>\varepsilon$, meaning that $\lambda_{uk}=\lambda_{lk}=0$. Using the explicit expression for $\boldsymbol{D}(\boldsymbol{x})$, given in Section 2, one concludes that (24) results in

$$\left(\frac{8\pi\mu\ell_k}{x_k^2}q_k^2\right)\frac{1}{\ell_k x_k^\sigma}=\sigma\lambda_V.$$

The expression within the bracket is the dissipation and the right hand side is constant for all k. Direct conclusions from this equation are:

(1) The dissipation per unit "generalized volume" $\ell_k x_k^\sigma$ is constant, i.e, has the same value in all pipes.

(2) $q_k^2\propto x_k^{2+\sigma}$, meaning that $q_k\propto r_k^{2+\sigma}$, where r_k is the radius of a pipe.

These conclusions hold for k such that $\bar{x}_k>x_k>\varepsilon$. When $\sigma=1$ the second conclusion is the cube law of Murray [14] first presented in 1926 as a result of physiological reasoning. It is a remarkable fact that this law reappear in the analysis performed here. Moreover, we have generalized this law to values of $\sigma\neq 1$.

Investigating Hagen–Poiseuille flow more closely one finds that the shear stress on the tube wall from the fluid is proportional to the ratio q_k/r_k^3. Thus, we may add to our two conclusions above:

(3) For all pipes k such that $\bar{x}_k>x_k>\varepsilon$ the shear stress on the tube wall from the fluid is constant when $\sigma=1$.Murray's law gives a condition on how bifurcation of pipes must occur. Consider, for instance, a pipe with flow q_1 that bifurcates into two pipes with flow q_2 and q_3, respectively (see Fig. 3). Since by Kirchhoff's law $q_1=q_2+q_3$, our generalized version of Murray's law implies

$$r_1^\gamma=r_2^\gamma+r_3^\gamma, \tag{28}$$

[4] However, unless $\Omega^*(0)$ is a singleton, we have not proven that *all* solutions to $(\mathscr{P})_0$ can be reached, (since we have not established that the solution set map is *lower* semi-continuous at 0).

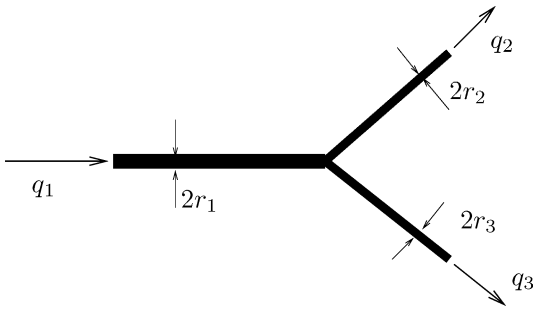

Fig. 3. A bifurcation of pipes.

where the "bifurcation exponent" $\gamma = 2 + \sigma$. Values other than 3 for this exponent has been reported in the literature. The value 2.55 is given in [15] while in [22] it is indicated that for the aorta a value of 2 may be appropriate, although the original value of 3 holds for peripheral regions of the arterial tree.

5. Algorithm

The numerical solution of the optimization problem $(\mathscr{P})_\varepsilon$ will be obtained by using a well known strategy from structural optimization, namely *separable convex approximation* [11], which in a special case turns out to be equivalent to an *optimality criteria method* [12]. Separable convex approximation implies, as a first step, to introduce an approximation of the original problem, which is solved as a step in an iterative strategy (cf. Fig. 4). The approximation involves a linearization of the original functions in terms of a conveniently chosen intermediate variable. As a preparatory for this step we change the independent variables in $(\mathscr{P})_\varepsilon$ from x_k to $y_k = x_k^\sigma$, equivalently written $\boldsymbol{x} = \tilde{\boldsymbol{x}}(\boldsymbol{y})$, the reason being that the constraints of $(\mathscr{P})_\varepsilon$ then become linear and are easily treated. Next, we chose to linearize $\tilde{\varphi}(\boldsymbol{y}) = \varphi(\tilde{\boldsymbol{x}}(\boldsymbol{y}))$ in the variables y_k^{-a}, where $a > 0$ will turn out to be related to a damping of the algorithm. Linearizing around the point $(\boldsymbol{y}^j)^\top = (y_1^{(j)}, \ldots, y_m^{(j)})$, we get the approximation

$$\tilde{\varphi}(\boldsymbol{y}) \approx \sum_{k=1}^{m} b_k^{(j)} y_k^{-a} + \text{constant}, \tag{29}$$

1. At the design $\boldsymbol{y}^{(j)}$, solve for the state $\boldsymbol{p}^{(j)}$.
2. Approximate $(\mathcal{P})_\varepsilon$ as a **convex** and **separable** explicit optimization problem $(\mathcal{P})_\varepsilon^j$.
3. Solve $(\mathcal{P})_\varepsilon^j$ by Lagrangian duality.
4. Solution to $(\mathcal{P})_\varepsilon^j$ defines new iterate $\boldsymbol{y}^{(j+1)}$.

Fig. 4. Scheme of sequential separable and convex programming.

where

$$b_k^{(j)} = \frac{\partial \tilde{\varphi}(\boldsymbol{y}^j)}{\partial (y_k^{-a})} = -\frac{(y_k^{(j)})^{1+a}}{a}\frac{\partial \tilde{\varphi}(\boldsymbol{y}^j)}{\partial y_k} = \frac{(y_k^{(j)})^{(2/\sigma)+a}}{8a\sigma\pi\mu\ell_k}(\boldsymbol{\gamma}_k^\top \boldsymbol{p}(\tilde{\boldsymbol{x}}(\boldsymbol{y}^j)) + f_k\ell_k)^2.$$

The last expression is obtained from (23).

Thus, we may state the following approximation of $(\mathscr{P})_\varepsilon$:

$$(\mathscr{P})_\varepsilon^j \begin{cases} \min\limits_{\boldsymbol{y}} & \sum_{k=1}^m b_k^{(j)} y_k^{-a}, \\ \text{subject to} & \sum_{k=1}^m \ell_k y_k \leqslant V, \quad \bar{\boldsymbol{y}} \geqslant \boldsymbol{y} \geqslant \epsilon\mathbf{1}, \end{cases}$$

where $\bar{y}_k = \bar{x}_k^\sigma$ for all k and $\epsilon = \varepsilon^\sigma$.

Problem $(\mathscr{P})_\varepsilon^j$ is separable and may be conveniently solved by duality where the first constraint (generalized volume) is relaxed. That is, a dual objective function is defined by

$$\varphi^*(\lambda) = \min_{\boldsymbol{y}} \{\mathscr{L}(\boldsymbol{y}, \lambda) | \boldsymbol{y} \geqslant \boldsymbol{y} \geqslant \epsilon\mathbf{1}\}, \tag{30}$$

where the Lagrangian function is

$$\mathscr{L}(\boldsymbol{y}, \lambda) = \sum_{k=1}^m b_k^{(j)} y_k^{-a} + \lambda\left(\sum_{k=1}^m \ell_k y_k - V\right).$$

It turns out that the min in (30) is obtained when

$$y_k(\lambda) = \begin{cases} \epsilon & \text{if} \quad \left(\dfrac{ab_k^{(j)}}{\lambda\ell_k}\right)^{1/(1+a)} < \epsilon, \\ \left(\dfrac{ab_k^{(j)}}{\lambda\ell_k}\right)^{1/(1+a)} & \text{if} \quad \epsilon \leqslant \left(\dfrac{ab_k^{(j)}}{\lambda\ell_k}\right)^{1/(1+a)} \leqslant \bar{y}_k, \\ \bar{y}_k & \text{if} \quad \left(\dfrac{ab_k^{(j)}}{\lambda\ell_k}\right)^{1/(1+a)} > \bar{y}_k \end{cases} \tag{31}$$

and the optimum of the dual problem is achieved when

$$\sum_{k=1}^m \ell_k y_k(\lambda) = V. \tag{32}$$

The volume constraint must be fulfilled with equality if $b_k^{(j)} > 0$ for all k (which can be expected in most situations in practice). In general $b_k^{(j)} \geqslant 0$, in which case there could be multiple solutions to $(\mathscr{P})_\varepsilon^j$. At least one of these, however, satisfies the volume constraint with equality.

We write η for the expression $1/(1+a)$ appearing as a "damping exponent" in (31). Numerical experiments representing the effect of the value of η on convergence behavior are reported in Section 6. Summarizing, the computational optimization algorithm that we have implemented becomes:

1. Solve the state problem to obtain $\boldsymbol{p}^{(j)} = \boldsymbol{p}(\tilde{\boldsymbol{x}}(\boldsymbol{y}^{(j)}))$.
2. Calculate the dissipation in each pipe,

$$d_k^{(j)} = \frac{(\boldsymbol{\gamma}_k^\top \boldsymbol{p}^{(j)} + f_k\ell_k)^2 (x_k^{(j)})^2}{8\pi\mu\ell_k}, \quad x_k^{(j)} = (y_k^{(j)})^{1/\sigma}, \ \ k = 1, \ldots, m.$$

3. Update the design to obtain $\boldsymbol{y}^{(j+1)}$: Let, for $k = 1, \ldots, m$,

$$\tilde{y}_k^{(j+1)} = y_k^{(j)} \left(\frac{d_k^{(j)}}{\sigma \lambda \ell_k y_k^{(j)}} \right)^{\eta}$$

and then $y_k^{(j+1)} = \tilde{y}_k^{(j+1)}$ unless $\tilde{y}_k^{(j+1)} < \epsilon$, then $y_k^{(j+1)} = \epsilon$, and unless $\tilde{y}_k^{(j+1)} > \bar{y}_k$, then $y_k^{(j+1)} = \bar{y}_k$, and
4. λ is determined using one-dimensional bisection such that $\boldsymbol{y}^{(j+1)}$ satisfies (32).
5. Check if the change in objective function value is below a prescribed tolerance. If not, go to step 1.

Finally the (locally) optimal radii become

$$r_k = (y_k^{(\infty)})^{1/2\sigma}/\sqrt{\pi}, \quad k = 1, \ldots, m.$$

It should be noted that step 1 is completely dominating the computational time. The update formula in step 3 is obtained by substituting $b_k^{(j)}$ into (31).

6. Numerical examples

This section contains four subsections. In Section 6.1 we study by means of small examples the effect of non-convexity. In Section 6.2 larger networks whose optimal solutions resembles arterial trees are studied. Section 6.3 contains an investigation of the influence of volume forces. Finally, in Section 6.4 the influence of using a generalized volume constraint, i.e., varying the parameter σ, is studied.

6.1. Consequences of non-convexity

As previously pointed out, the function φ is non-convex. So even for $\sigma = 1$, which represents convex constraints, $(\mathscr{P})_\varepsilon$ is a non-convex problem. Thus, we may investigate the possibility of multiple local optima.

In Fig. 5 three very simple ground structures are shown in the upper part and corresponding global optima are shown in the lower part. Arrows indicate inflow and outflow: in the upper part of the figure only prescribed flows are shown which are all taken to be of unit magnitude. The left hand example has a global optimum which consists of just one of the three pipes having an area different from zero. In the middle example the prescribed flow is of different sign and another global optimum is obtained. In the right hand example, two of the pipes in the ground structure are made longer. This changes the character of the global solution as shown in the figure. However, the symmetric distribution of area, that was a global optimum in the middle example, is still a local optimum. Since our algorithm is local in character it may end up in any of the (at least) two optima depending on what distribution of areas is taken as a starting point.

Next a slightly larger, but still small-size, example is studied to investigate the possibility of local optima. In Fig. 6 a ground structure with equal initial distribution of areas is shown to the left and the numerically obtained solution is to the right. There is one node with prescribed pressure on the top and two nodes with equal prescribed outflow on the bottom. In Fig. 7 a ground structure with unequal distribution of areas is shown to the left. That is, the starting point for the algorithm is different from that used in the example of Fig. 6, but the boundary conditions are equal. The corresponding solution is shown to the right in Fig. 7. The objective function value for the solution in Fig. 7 is 1.64 times better than the solution in Fig. 6. An analytical investigation of a similar problem in [5] shows that the solution in Fig. 7 is a global optimum.

A conclusion to be drawn from these examples seems to be that local optima correspond to networks consisting of more pipes than corresponding global optima. This is indicated also from the equations since a large pipe gives less resistance to flow than two smaller ones carrying the same total volume.

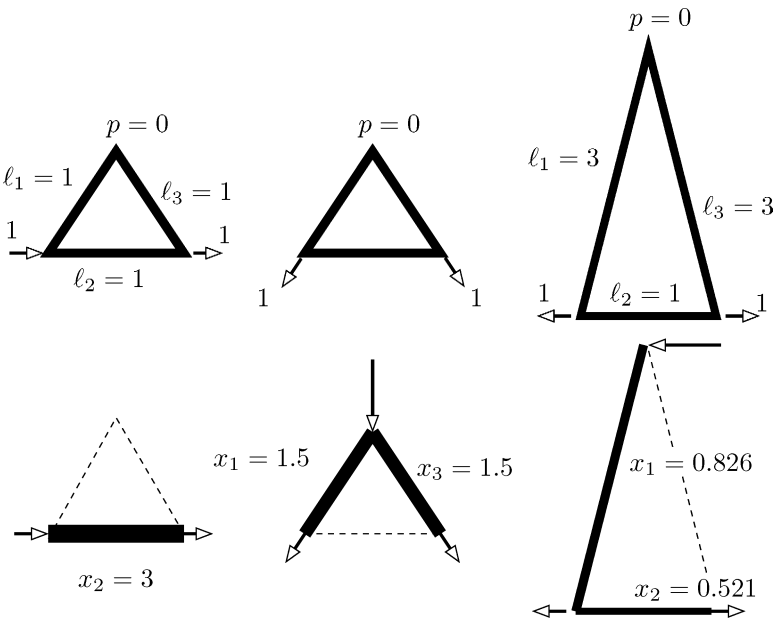

Fig. 5. Global optima for very small networks.

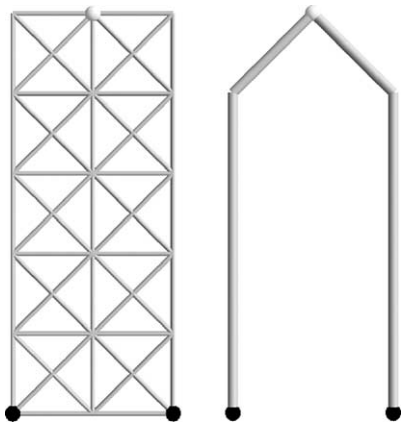

Fig. 6. Ground structure with uniform initial cross-sectional areas to the left. Non-global local optimum to the right.

6.2. Arterial tree-type networks

By an arterial tree-type network we mean a network having one or two nodes with prescribed pressure and a large number of nodes with prescribed flow. In the case of two nodes with prescribed pressure, these pressures are set equal, and we treat in this subsection the case $\boldsymbol{f} = \boldsymbol{0}$, so according to item 1 of Section 3 we are minimizing dissipation. Furthermore, the prescribed flow is uniform so we are also satisfying the condition of the special case 2 in Section 3. This means, by Eq. (21), that the values of prescribed pressure and flow, p_{fix} and Q_{out}, are unimportant for the result. Even further, the self-similarity indicated at the end of Section 3 shows that the value of prescribed volume, V, also has no influence on the appearance of optimal networks.

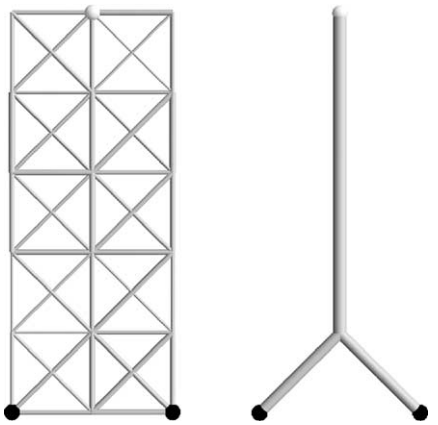

Fig. 7. Ground structure with non-uniform initial cross-sectional areas to the left. The optimum to the right is a global one.

The ground structure of an arterial tree-type network is generated in a random fashion. A region in the plane or in space is first chosen. In the problems solved here this region is taken as the area of a circle, part of such an area or the volume between concentric spheres. Fig. 8 shows three ground structure based on these geometric figures.

A prescribed number of nodes is randomly distributed within the allowed domain one by one. If the distance between a new node and an already existing node is less than a value $\ell_{\min}$, then the new node is not

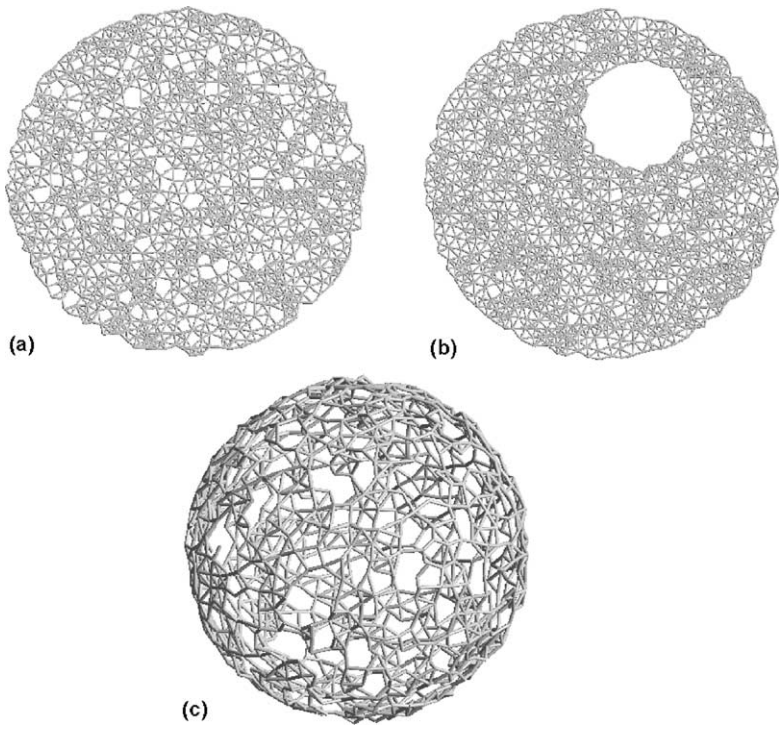

Fig. 8. Ground structures for arterial tree-type networks. Upper left, (a), is constructed on a circular area; upper right, (b), is constructed on part of such a circular area and the lower ground structure, (c), has a spherical shape.

accepted. In the examples shown here, one or two of the nodes have prescribed pressure, i.e., belong to β, and the rest of the nodes have a uniform prescribed flow, i.e., belong to γ. However, it is also possible to prescribe the flow to zero for a fraction of the γ-nodes, to allow for bifurcation of the tree without associated outflow. Pipes between nodes are generated by specifying a value $\ell_{\max}$: if the distance between two nodes is less then this value then the two nodes are connected by a pipe.

In Fig. 9 the result based on the upper left ground structure of Fig. 8, i.e., (a), is shown. Here we have one node with prescribed pressure and 499 randomly distributed nodes with uniform prescribed flow. The radius of the circle is 0.5 and $\ell_{\min} = 0.019$. Pipes are generated on the basis of $\ell_{\max} = 0.044$, which resulted in 3206 segments in the ground structure. The maximum volume is given by $V = 0.003$, but as indicated above, due to self-similarity this value is unimportant for the shape of the optimum network. The value of the volume exponent is $\sigma = 1$ and in the algorithm a damping exponent $\eta = 0.2$ was used. The result in Fig. 9 was generated after 54 iterations of the algorithm, when using as convergence measure a relative change in objective function value of 0.1×10^{-7}. This numerical value was used the check convergence in all subsequent calculations. Comparing the result of Fig. 9 with those of Figs. 6 and 7 one is inclined to say that Fig. 9 probably shows a local optimum.

For the ground structure shown in Fig. 8(a) we have also investigated the influence of the damping coefficient η on the algorithmic behavior. The problem was run for $\eta = 0.1$, 0.2, 0.3, 0.5, 0.6 and 0.7. The number of required iterations for the first five cases was 115, 54, 36, 23 and 36, while for $\eta = 0.7$ the algorithm did not converge. The objective function values at convergence coincided to the third digit. Visually, the optimal trees where indistinguishable except for $\eta = 0.6$ where a slight difference was noticed. Our interpretation of this is that for such a large value of the damping coefficient a nearby local optimum was found.

In Fig. 10 the result based on the upper right ground structure of Fig. 8, i.e., (b), is shown. Here we have two nodes with prescribed equal pressure and 998 nodes with prescribed flow. Other numerical values are $\ell_{\min} = 0.019$, $\ell_{\max} = 0.044$, $V = 0.003$, $\sigma = 1$ and $\eta = 0.2$ and the number of segments is 3440. The arterial tree decouples into two separate trees, each one being "supported" by one pressure node. The result was obtained after 57 iterations.

In Fig. 11 the result based on the lower three-dimensional ground structure of Fig. 8, i.e., (c), is shown. Again, we have two nodes with prescribed equal pressure and 998 nodes with prescribed flow. Other nu-

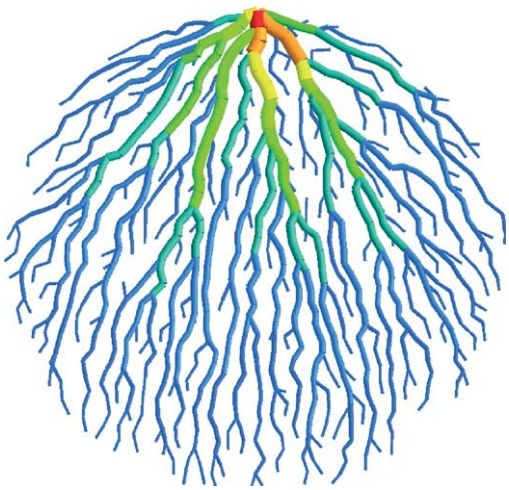

Fig. 9. Arterial tree-type two-dimensional network. This solution is likely to be a local optimum.

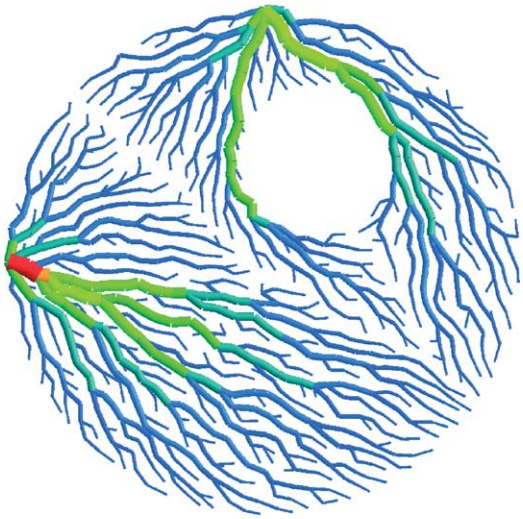

Fig. 10. Arterial tree-type two-dimensional network with two nodes with prescribed pressure.

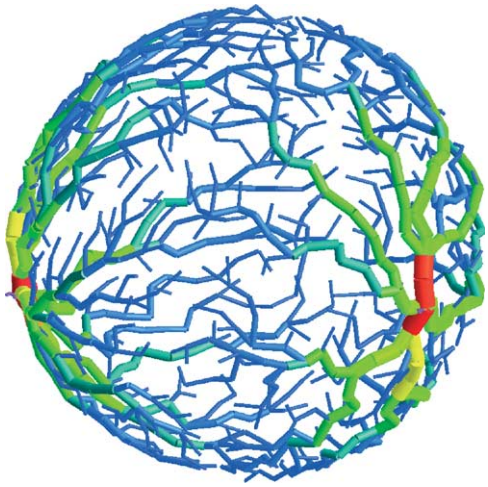

Fig. 11. Arterial tree-type three-dimensional network with two nodes with prescribed pressure.

merical values are $\ell_{\min} = 0.032$, $\ell_{\max} = 0.07$, $V = 0.01$, $\sigma = 1$ and $\eta = 0.2$ and the number of segments is 3832. As in Fig. 10 the arterial tree decouples into two separate trees. The result was obtained after 54 iterations.

6.3. An example with non-zero volume force

To study the effect of a non-zero volume force $\boldsymbol{f}$ we have considered the regular ground structure shown in Fig. 12. The pressure is prescribed in the corner nodes and the flow is prescribed to zero in all other nodes. That is, we are in the situation of expressed by item 3 and Eq. (22) of Section 3. Eq. (22) contains two terms. Depending on the relative magnitude of $\bar{\boldsymbol{p}}_\beta$ and $\boldsymbol{f}$ different optimum solutions will be obtained. We have investigated this by fixing prescribed pressures to the value 1 at the two corner nodes to the right and

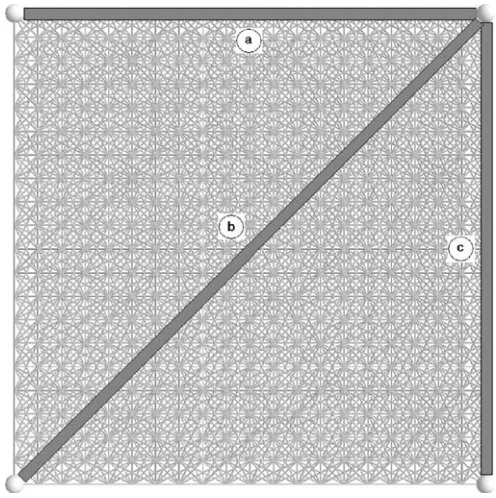

Fig. 12. Ground structure used for study of effect of volume force. Three different optimal solutions, depending on the value of the volume force, are shown.

to the value 2 at the two corner nodes to the left and then varying the value of $\boldsymbol{f}$. Three values for the force in the upward vertical direction are tested, $f^1_{\text{vertical}} = 0.1$, $f^2_{\text{vertical}} = 1.0$ and $f^3_{\text{vertical}} = 10$, while the force in the horizontal direction is zero. For f^1_{vertical} the second term in (22), i.e., the force, has no influence on the optimal solution, which we find to be just one pipe (or rather a composition of smaller equal pipes) going from the upper left hand pressure node to the upper right hand pressure node, shown as **a** in Fig. 12. It is obvious that another solution of this problem with the same objective function value is a pipe that goes between the two lower pressure nodes. Next, for f^2_{vertical} the two terms in (22) are equally important: the solution is an inclined pipe going from upper right hand pressure node to the lower left hand pressure node, shown as **b** in Fig. 12. Finally, for f^3_{vertical} the second term in (22) dominates and the solution is a pipe that goes vertically between the two right hand pressure nodes, shown as **c** in Fig. 12.

6.4. The effect of σ

All of the previous calculations are done for the value $\sigma = 1$, i.e., for a standard volume constraint. Changing σ to another value, i.e., changing how cost of volume is counted, should change the appearance of the optimal tree, as is evident from Murray's bifurcation equation (28). To get a feeling for the general tendencies of this change, we study a very simple two-pipe problem, shown in Fig. 13. It consists of three nodes and two pipes. The outflow is prescribed to $Q_1^{\text{out}} > 0$ and $Q_2^{\text{out}} > 0$ at the two right hand nodes and a pressure p is prescribed at the left hand node. In each pipe the flow is q_1 and q_2, respectively. Kirchhoff's law says that $q_1 = Q_1^{\text{out}} + q_2$ and $q_2 = Q_2^{\text{out}}$. Optimal radii of the pipes satisfy Murray's law, $q_k \propto r_k^\gamma$, where $\gamma = 2 + \sigma$ and r_k is the optimal radius of pipe k. Combining these equations results in

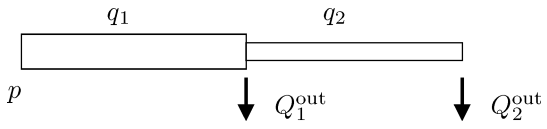

Fig. 13. A two-pipe arterial tree-type structure.

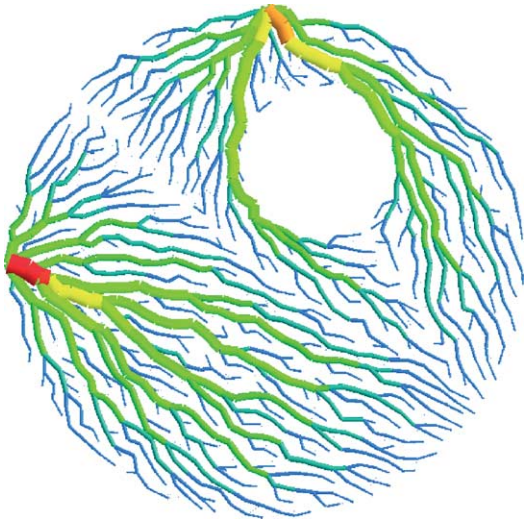

Fig. 14. Arterial tree-type two-dimensional network with two nodes with prescribed pressure ($\sigma = 1/2$).

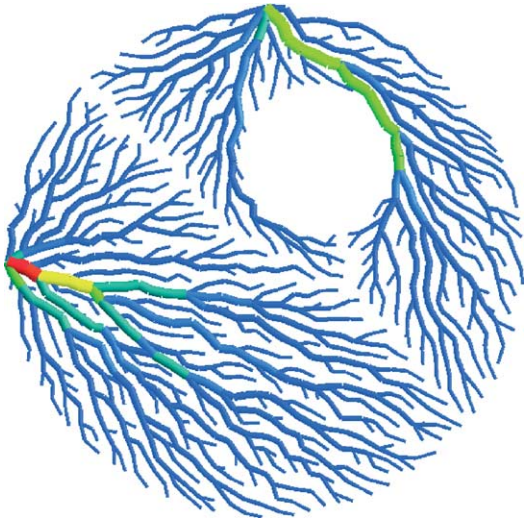

Fig. 15. Arterial tree-type two-dimensional network with two nodes with prescribed pressure ($\sigma = 2$).

$$\left(\frac{r_1}{r_2}\right)^{\gamma} = \frac{Q_1^{\text{out}}}{Q_2^{\text{out}}} + 1.$$

The right hand side is constant and independent of γ and since it is larger than 1 it holds that $r_1 > r_2$. Furthermore, one concludes that a large value of γ gives a smaller quotient r_1/r_2 and conversely. Guessing that this conclusion can be generalized to larger arterial tree-like networks, we may say that a large value of σ should give networks with more equal radii than what a small value of σ gives. This is confirmed by our numerical calculations presented in Figs. 14 and 15. In these figures the problem based on ground structure (b) in Fig. 8 is recalculated with values $\sigma = 1/2$ and $\sigma = 2$. The result for $\sigma = 1$ was shown in Fig. 10. For $\sigma \neq 1$ the volume of the structure is not constant through iterations and can not be prescribed beforehand.

However, for visual comparison the results in Figs. 10, 14 and 15 have been scaled to the same total volume. Note that $\sigma = 2$ is the critical value which makes the state equation linear in the variables $y_k = x_k^\sigma$. Thus, for this value of σ the optimization problem is convex. However, this did not make it easier to achieve convergence. In fact, 606 iterations was required to obtain Fig. 15, to be compared with 32 for 14, requiring the same tolerance.

7. Further work

The present paper extends and applies techniques from the area of truss topology optimization to flow networks. It is a first study in this direction and there is a very large number of possible extensions and applications. We indicate a few of these here: (i) The difficulty related to con-convexity of the optimization problem should be addressed. Filter techniques (see [20]) may be tested. We can also imagine an approach where a god initial design (starting point) is generated by gradually expanding (growing) a tree structure. (ii) In many applications there may be a small head loss at each bifurcation that is not resolved in the present model. An extension in this direction could follow recent work on frame topology optimization [13]. (iii) A non-linear state problem, where the viscous resistance depends on the Reynold's number, could easily be extended to. In relation to bio-mechanics applications we remark that there are indications that turbulence may occur in the aorta. (iv) Examples in which a closed network is studied are of interest. In a bio-mechanics context this would correspond to arteries and veins.

Appendix A. Proof of Proposition 6

A.1. Preliminaries

A.1.1. The state problem formulated as optimization problems

Previously the minimization principle (14) was stated. This minimization problem is equivalent to the state problem (13), and it is stated in the pressures $\boldsymbol{p}$. We now give another minimization problem, $(\mathscr{C})(\boldsymbol{x})$, stated in the volume flows $\boldsymbol{q}$, which we show is also equivalent to (13), so (14) and $(\mathscr{C})(\boldsymbol{x})$ can be considered a dual pair of optimization problems.

In the simplified case of no volume forces and only zero-prescribed pressures, the optimization problem $(\mathscr{C})(\boldsymbol{x})$ states that the flows in the segments are those that satisfy Kirchoff's law, i.e. balance of flow at all nodes where nodal inflows are known, and that minimize the dissipated power. In the general case the problem reads

$$(\mathscr{C})(\boldsymbol{x})\begin{cases}\min\limits_{q_k} & \sum_k q_k\left(\dfrac{q_k}{2D_k(x_k)} - f_k\ell_k - \bar{\boldsymbol{p}}_\beta^\top(\boldsymbol{\gamma}_k)_\beta\right),\\ \text{subject to} & \sum_k q_k(\boldsymbol{\gamma}_k)_\alpha = \overline{\boldsymbol{Q}}_\alpha\end{cases}$$

in which the minimization is performed over all q_k's corresponding to active segments, i.e., all indices k such that $x_k > 0$, equivalently written $k \in I(\boldsymbol{x})$. It is also understood that the summations $\sum_k$ are sums over all $k \in I(\boldsymbol{x})$. Hence, segments for which $x_k = 0$ do not enter the problem statement and do not contribute to dissipation power. For indices $k \notin I(\boldsymbol{x})$ we take $q_k = 0$, i.e., there is zero flow if there is no pipe.

Given a collection of cross-section areas, i.e. a design $\boldsymbol{x}$, suppose there is at least one collection of segment flows q_k, $k \in I(\boldsymbol{x})$, such that

$$\sum_k q_k(\boldsymbol{\gamma}_k)_\alpha = \overline{\boldsymbol{Q}}_\alpha. \tag{A.1}$$

(If not, no matter what constitutive properties the fluid has, there is no way the network can produce a flow that satisfies the prescribed $\overline{\boldsymbol{Q}}_\alpha$. This happens for instance if $\boldsymbol{x} = \boldsymbol{0}$, $\overline{\boldsymbol{Q}}_\alpha \neq \boldsymbol{0}$.) Then, the feasible set of $(\mathscr{C})(\boldsymbol{x})$ is non-empty, so there exists a unique solution to $(\mathscr{C})(\boldsymbol{x})$ since the objective is strictly convex, coercive (i.e. the function goes to infinity if the norm of the argument goes to infinity) and lower semi-continuous (i.e. for any convergent sequence of arguments, lim inf of the function is bounded below by the function value evaluated at the limit). Since the constraints are linear, the Abadie constraint qualification is valid (cf. Lemma 5.1.4 in [3]), and therefore the KKT conditions are necessary for optimality (see e.g. Theorem 5.1.3 in [3]). Since the problem is convex these are also sufficient (cf. Theorem 4.2.16 in [3]). To find the KKT conditions, form the Lagrangian

$$\mathscr{L}(\{q_k\}_{k\in I(\boldsymbol{x})}, \boldsymbol{p}_\alpha) = \sum_k q_k \left(\frac{q_k}{2D_k(x_k)} - f_k \ell_k - \bar{\boldsymbol{p}}_\beta^\top (\boldsymbol{\gamma}_k)_\beta \right) - \boldsymbol{p}_\alpha^\top \left(\sum_k q_k (\boldsymbol{\gamma}_k)_\alpha - \overline{\boldsymbol{Q}}_\alpha \right),$$

where $\boldsymbol{p}$ is an n-vector such that $\boldsymbol{p}_\alpha$ are the Lagrangian multipliers. The stationarity is obtained by taking the derivative of $\mathscr{L}$ with respect to all q_k's and setting these expressions equal to zero:

$$\frac{\partial \mathscr{L}(\{q_k\}_{k\in I(\boldsymbol{x})}, \boldsymbol{p}_\alpha)}{\partial q_k} = \frac{q_k}{D_k(x_k)} - f_k \ell_k - \bar{\boldsymbol{p}}_\beta^\top (\boldsymbol{\gamma}_k)_\beta - \boldsymbol{p}_\alpha^\top (\boldsymbol{\gamma}_k)_\alpha = 0, \quad \forall i \in I(\boldsymbol{x}) \tag{A.2}$$

or equivalently

$$q_k = D_k(x_k)\left(f_k \ell_k + \boldsymbol{p}^\top \boldsymbol{\gamma}_k\right); \boldsymbol{p}_\beta = \bar{\boldsymbol{p}}_\beta, \quad \forall k \in I(\boldsymbol{x}). \tag{A.3}$$

A collection of segment flows q_k, $k \in I(\boldsymbol{x})$ solves $(\mathscr{C})(\boldsymbol{x})$ if and only if feasibility (A.1) and stationarity (A.3) hold. These are in fact equivalent to the state problem (13).

First, assume feasibility (A.1) and stationarity (A.3) hold and define

$$\boldsymbol{Q} = \sum_k D_k(x_k)(f_k \ell_k + \boldsymbol{p}^\top \boldsymbol{\gamma}_k)\boldsymbol{\gamma}_k. \tag{A.4}$$

Inserting (A.3) into (A.1) yields

$$\sum_k D_k(x_k)(f_k \ell_k + \boldsymbol{p}^\top \boldsymbol{\gamma}_k)(\boldsymbol{\gamma}_k)_\alpha = \overline{\boldsymbol{Q}}_\alpha,$$

so it follows that $\boldsymbol{Q}_\alpha = \overline{\boldsymbol{Q}}_\alpha$ and

$$\boldsymbol{Q} = \sum_{k=1}^{m} D_k(x_k)(f_k \ell_k + \boldsymbol{p}^\top \boldsymbol{\gamma}_k)\boldsymbol{\gamma}_k = \boldsymbol{B}^\top \boldsymbol{D}(\boldsymbol{x})(\boldsymbol{B}\boldsymbol{p} + \boldsymbol{f})$$

since $D_k(0) = 0$. The relation $\boldsymbol{p}_\beta = \bar{\boldsymbol{p}}_\beta$ is already satisfied in (A.3), and so everything in (13) holds.

Now assume, conversely, that (13) holds. Defining $q_k = D_k(x_k)(f_k \ell_k + \boldsymbol{p}^\top \boldsymbol{\gamma}_k)$ for all $k \in I(\boldsymbol{x})$, stationarity (A.3) is automatically satisfied, and feasibility (A.1) follows from $\boldsymbol{B}^\top \boldsymbol{D}(\boldsymbol{x})(\boldsymbol{B}\boldsymbol{p} + \boldsymbol{f}) = \boldsymbol{Q}$.

We can now conclude the following primal-dual relation: If the feasible set of $(\mathscr{C})(\boldsymbol{x})$ is non-empty, then there exists a unique solution q_k, $k \in I(\boldsymbol{x})$, to $(\mathscr{C})(\boldsymbol{x})$ and there exists at least one vector of multipliers $\boldsymbol{p}_\alpha$ such that (A.3) holds and such that $\boldsymbol{p}$ solves (14). Conversely, if $\boldsymbol{p}$ solves (14), then defining $q_k = D_k(x_k)(f_k \ell_k + \boldsymbol{p}^\top \boldsymbol{\gamma}_k)$, $k \in I(\boldsymbol{x})$, these solve $(\mathscr{C})(\boldsymbol{x})$.

A.1.2. Definitions of $\varphi(\boldsymbol{x})$

Previously the objective function $\varphi(\boldsymbol{x})$ was defined in (15) which is equivalent to

$$\varphi(\boldsymbol{x}) = \sup_{\boldsymbol{p}\in\mathscr{P}} \left(\overline{\boldsymbol{Q}}_\alpha^\top \boldsymbol{p}_\alpha - \tfrac{1}{2}(\boldsymbol{B}\boldsymbol{p} + \boldsymbol{f})^\top \boldsymbol{D}(\boldsymbol{x})(\boldsymbol{B}\boldsymbol{p} + \boldsymbol{f}) \right). \tag{A.5}$$

Suppose $\boldsymbol{x}$ is a design for which the feasible set of $(\mathscr{C})(\boldsymbol{x})$ is non-empty, or equivalently, for which there exist solutions to the state problem. Then we know that the expression (17) holds. We next present an alternative, equivalent, definition of $\varphi(\boldsymbol{x})$ that will prove to be useful for the investigation of continuity properties.

The unique solution to $(\mathscr{C})(\boldsymbol{x})$ is denoted $q_k(\boldsymbol{x})$, $k \in I(\boldsymbol{x})$, and we can then define $\varphi(\boldsymbol{x})$ as

$$\varphi(\boldsymbol{x}) = \sum_k q_k(\boldsymbol{x}) \left(\frac{q_k(\boldsymbol{x})}{2D_k(x_k)} - f_k \ell_k - \bar{\boldsymbol{p}}_\beta^\top (\gamma_k)_\beta \right). \tag{A.6}$$

From $(\mathscr{C})(\boldsymbol{x})$ we understand that we can also write

$$\varphi(\boldsymbol{x}) = \inf \sum_k q_k \left(\frac{q_k}{2D_k(x_k)} - f_k \ell_k - \bar{\boldsymbol{p}}_\beta^\top (\gamma_k)_\beta \right) \tag{A.7}$$

in which the infimum is taken over all q_k, $k \in I(\boldsymbol{x})$, such that (A.1) holds. (If the feasible set of $(\mathscr{C})(\boldsymbol{x})$ is empty, or equivalently if there are no state problem solutions, then we can naturally define $\varphi(\boldsymbol{x}) = +\infty$). Using (A.2) in (A.6) and $q_k = 0$ for all $k \notin I(\boldsymbol{x})$, one obtains

$$\begin{aligned} \varphi(\boldsymbol{x}) &= \sum_k q_k(\boldsymbol{x}) \Big(-\tfrac{1}{2} f_k \ell_k - \tfrac{1}{2} \bar{\boldsymbol{p}}_\beta^\top (\gamma_k)_\beta + \tfrac{1}{2} \boldsymbol{p}_\alpha^\top(\boldsymbol{x}) (\gamma_k)_\alpha \Big) \\ &= -\tfrac{1}{2} \boldsymbol{f}^\top \boldsymbol{q}(\boldsymbol{x}) - \tfrac{1}{2} \bar{\boldsymbol{p}}_\beta^\top \sum_k q_k(\boldsymbol{x}) (\gamma_k)_\beta + \tfrac{1}{2} \boldsymbol{p}_\alpha^\top(\boldsymbol{x}) \sum_k q_k(\boldsymbol{x}) (\gamma_k)_\alpha, \end{aligned}$$

which simplifies to

$$\varphi(\boldsymbol{x}) = -\tfrac{1}{2} \boldsymbol{f}^\top \boldsymbol{q}(\boldsymbol{x}) - \tfrac{1}{2} \bar{\boldsymbol{p}}_\beta^\top \boldsymbol{Q}_\beta(\boldsymbol{x}) + \tfrac{1}{2} \boldsymbol{p}_\alpha^\top(\boldsymbol{x}) \overline{\boldsymbol{Q}}_\alpha$$

by (A.1) and (A.4). This expression coincides with (17), and therefore we have validated the alternative definition (A.7).

Whereas the expression (17) is the most accessible for the interpretation of $\varphi(\boldsymbol{x})$, (A.7) is useful for upper semi-continuity properties and (A.5) for lower semi-continuity.

A.2. Proof of the continuity with respect to the lower design bound

Now we prove the desired continuity for the minimization problem $(\mathscr{P})_\varepsilon$. We start by making a change of variables according to

$$x_k = y_k^{1/\sigma}, \quad k = 1, \ldots, m \Longleftrightarrow \boldsymbol{x} = \tilde{\boldsymbol{x}}(\boldsymbol{y}). \tag{A.8}$$

The optimization problem then becomes

$$(\widetilde{\mathscr{P}})_\varepsilon \begin{cases} \min\limits_{\boldsymbol{y}} & \varphi(\tilde{\boldsymbol{x}}(\boldsymbol{y})), \\ \text{subject to} & \sum_{k=1}^m \ell_k y_k \leqslant V, \quad \bar{\boldsymbol{y}} \geqslant \boldsymbol{y} \geqslant \varepsilon^\sigma \boldsymbol{1}, \end{cases}$$

where $\bar{y}_k = \bar{x}_k^\sigma$. Note that all constraints are linear after the change of variables.

It can be seen by standard arguments that $(\widetilde{\mathscr{P}})_\varepsilon$ has at least one solution $\boldsymbol{y}^*(\varepsilon)$ for any $\varepsilon > 0$ sufficiently small for the feasible set to be non-empty. (This follows from the compactness of the feasible design domain and lower semi-continuity of $\boldsymbol{y} \mapsto \varphi(\tilde{\boldsymbol{x}}(\boldsymbol{y}))$ which follows immediately from (A.5)). Since the feasible sets of $(\widetilde{\mathscr{P}})_\varepsilon$ are uniformly bounded and closed as $\varepsilon \to 0$, it follows that there is a vector $\boldsymbol{y}^*$ such that $\boldsymbol{y}^*(\varepsilon) \to \boldsymbol{y}^*$ for some subsequence. We let $\{\boldsymbol{y}^*(\varepsilon)\}$ denote any such convergent subsequence. It is clear that $\boldsymbol{y}^*$ is feasible in $(\widetilde{\mathscr{P}})_0$. We will prove that $\boldsymbol{y}^*$ is also optimal in $(\widetilde{\mathscr{P}})_0$, and thereby establish the desired continuity result as well as existence of solutions to $(\mathscr{P})_0$.

Let $\boldsymbol{y}$ be any feasible design vector in $(\widetilde{\mathscr{P}})_0$ for which there are state problem solutions. The feasible region of $(\widetilde{\mathscr{P}})_\varepsilon$ is non-empty for all sufficiently small $\varepsilon > 0$. Moreover it is defined by linear constraints and it is closed and convex. We can then consider the Euclidean projection of $\boldsymbol{y}$ onto this set, resulting in the point $\boldsymbol{y}(\varepsilon)$, and can characterize the projection as a quadratic program where the objective equals $\frac{1}{2}\|\boldsymbol{y} - \cdot\|^2$ and the feasible set is that of $(\widetilde{\mathscr{P}})_\varepsilon$. It is then possible to apply the stability results for definite quadratic programs established in [10]. This results in

$$\|\boldsymbol{y}(\varepsilon) - \boldsymbol{y}\| \leqslant C\varepsilon^\sigma \tag{A.9}$$

for some $C > 0$ independent of ε and for all sufficiently small ε.

Since $\boldsymbol{y}^*(\varepsilon)$ solves $(\widetilde{\mathscr{P}})_\varepsilon$ and $\boldsymbol{y}(\varepsilon)$ is feasible in $(\widetilde{\mathscr{P}})_\varepsilon$, we get

$$\varphi(\tilde{\boldsymbol{x}}(\boldsymbol{y}^*(\varepsilon))) \leqslant \varphi(\tilde{\boldsymbol{x}}(\boldsymbol{y}(\varepsilon))). \tag{A.10}$$

We will next take lim inf and use the sup characterization (A.5) in the left hand side of (A.10) and lim sup and use the inf characterization (A.7) in the right hand side. Moreover, suplim inf is smaller than or equal to lim inf sup, so

$$\begin{aligned}
&\sup_{\boldsymbol{p}\in\mathscr{P}} \liminf_{\varepsilon\to 0}\left(\overline{\boldsymbol{Q}}_\alpha^\top \boldsymbol{p}_\alpha - \tfrac{1}{2}(\boldsymbol{B}\boldsymbol{p}+\boldsymbol{f})^\top \boldsymbol{D}(\tilde{\boldsymbol{x}}(\boldsymbol{y}^*(\varepsilon)))(\boldsymbol{B}\boldsymbol{p}+\boldsymbol{f})\right) \\
&\quad\leqslant \limsup_{\varepsilon\to 0} \inf_{q_k} \sum_{k=1}^m q_k\left(\frac{q_k}{2D_k(y_k(\varepsilon)^{1/\sigma})} - f_k\ell_k - \bar{\boldsymbol{p}}_\beta^\top(\gamma_k)_\beta\right).
\end{aligned} \tag{A.11}$$

The matrix $\boldsymbol{D}(\tilde{\boldsymbol{x}}(\boldsymbol{y}^*(\varepsilon)))$ converges to $\boldsymbol{D}(\tilde{\boldsymbol{x}}(\boldsymbol{y}^*))$ as $\varepsilon \to 0$, so, recalling (A.5), this yields

$$\varphi(\tilde{\boldsymbol{x}}(\boldsymbol{y}^*)) \leqslant \limsup_{\varepsilon\to 0} \inf_{q_k} \sum_{k=1}^m q_k\left(\frac{q_k}{2D_k(y_k(\varepsilon)^{1/\sigma})} - f_k\ell_k - \bar{\boldsymbol{p}}_\beta^\top(\gamma_k)_\beta\right). \tag{A.12}$$

Now let q_k, $k \in I(\boldsymbol{y})$, be any collection of flows such that (A.1) holds. Add $q_k = 0$ for all $k \notin I(\boldsymbol{y})$. Then we get q_k, $k = 1, \ldots, m$, such that

$$\sum_{k=1}^m q_k(\gamma_k)_\alpha = \overline{\boldsymbol{Q}}_\alpha$$

and can insert this in the right hand side of (A.12). This results in

$$\begin{aligned}
\varphi(\tilde{\boldsymbol{x}}(\boldsymbol{y}^*)) &\leqslant \limsup_{\varepsilon\to 0} \sum_{k\in I(\boldsymbol{y})} q_k\left(\frac{q_k}{2D_k(y_k(\varepsilon)^{1/\sigma})} - f_k\ell_k - \bar{\boldsymbol{p}}_\beta^\top(\gamma_k)_\beta\right) \\
&= \sum_{k\in I(\boldsymbol{y})} q_k\left(\frac{q_k}{2D_k(y_k^{1/\sigma})} - f_k\ell_k - \bar{\boldsymbol{p}}_\beta^\top(\gamma_k)_\beta\right) < +\infty,
\end{aligned} \tag{A.13}$$

where we have used (A.9), the continuity of $D_k(\cdot)$ and $y_k(\varepsilon) > 0$, $y_k > 0$ for all $k \in I(\boldsymbol{y})$. From this we see that there is at least one state of equilibrium for $\tilde{\boldsymbol{x}}(\boldsymbol{y}^*)$. Moreover, since (A.13) holds for all q_k, $k \in I(\boldsymbol{y})$, for which (A.1) is true, we can take the infimum over all such q_k's. By appealing to (A.7) this gives

$$\varphi(\tilde{\boldsymbol{x}}(\boldsymbol{y}^*)) \leqslant \varphi(\tilde{\boldsymbol{x}}(\boldsymbol{y})),$$

which proves that $\boldsymbol{y}^*$ is a solution to $(\widetilde{\mathscr{P}})_0$!

Concluding, if $\{\boldsymbol{x}^*(\varepsilon)\}$ denotes any sequence of globally optimal solutions to $(\mathscr{P})_\varepsilon$ as $\varepsilon \to 0$, then there exists a convergent subsequence, and for any such subsequential limit $\boldsymbol{x}^*$, it holds that $\boldsymbol{x}^*$ is a globally optimal solution to $(\mathscr{P})_0$.

References

[1] J.-P. Aubin, H. Frankowska, Set-Valued Analysis, Birkhäuser, Boston, 1990.
[2] M.S. Bazaraa, J.J. Jarvis, Linear Programming and Network Flows, John Wiley and Sons, New York, 1977.
[3] M.S. Bazaraa, H.D. Sherali, C.M. Shetty, Nonlinear Programming: Theory and Algorithms, John Wiley and Sons, New York, 1993.
[4] A. Bejan, Shape and Structure, from Engineering to Nature, Cambridge University Press, Cambridge, United Kingdom, 2000.
[5] A. Bejan, L.A.O. Rocha, S. Lorente, Thermodynamic optimization of geometry: T- and Y-shaped constructs of fluid streams, Int. J. Therm. Sci. 39 (2000) 949–960.
[6] M.P. Bendsøe, A. Ben-Tal, J. Zowe, Optimization methods for truss geometry and topology design, Struct. Optim. 7 (1994) 141–159.
[7] A. Ben-Tal, G. Eiger, J. Outrata, J. Zowe, A nondifferentiable approach to decomposable optimization problems with an application to the design of water distribution, in: Lecture Notes in Econom. and Math. Systems, vol. 382, Springer, Berlin, 1992.
[8] F.H. Clarke, Optimization and Nonsmooth Analysis, John Wiley, New York, 1983.
[9] J.B. Dennis, Mathematical Programming and Electrical Networks, MIT Press and John Wiley, New York, 1959.
[10] J.W. Daniel, Stability of the solution of definite quadratic programs, Math. Program. 5 (1973) 41–53.
[11] C. Fleury, CONLIN: an efficient dual optimizer based on convex approximation concepts, Struct. Optim. 1 (1989) 81–89.
[12] C. Fleury, Reconciliation of mathematical programming and optimality criteria approaches to structural optimization, in: A.J. Morris (Ed.), Foundations of Structural Optimization: A Unified Approach, Wiley, New York, 1982, pp. 363–404.
[13] H. Fredricson, T. Johansen, A. Klarbring, J. Petersson, Topology optimization of frame structures with flexible joints, Struct. Multidiscip. Optim., to appear.
[14] C.D. Murray, The physiological principle of minimum work. I. The vascular system and the cost of blood volume, Proc. Nat. Acad. Sci. 12 (1926) 207–214.
[15] W. Schreiner, P.F. Buxbaum, Computer-optimization of vascular trees, IEEE Trans. Biomed. Engrg. 40 (5) (1993) 482–491.
[16] W. Schreiner, F. Neumann, M. Neumann, A. End, S.M. Roedler, S. Aharinejad, The influence of optimization target selection on the structure of arterial tree models generated by constrained constructive optimization, J. General Physiol. 106 (1995) 583–599.
[17] R. Karch, F. Neumann, M. Neumann, W. Schreiner, A three-dimensional model for arterial tree representation, generated by constrained constructive optimization, Comput. Biol. Med. 29 (1999) 19–38.
[18] W. Prager, Problems of network flow, ZAMP 16 (1965) 185–190.
[19] A.P. Seyranian, Homogeneous functionals and structural optimization problems, Int. J. Solids Struct. 15 (1979) 749–759.
[20] O. Sigmund, J. Petersson, Numerical instabilities in topology optimization: A survey on procedures dealing with checkerboards, mesh-dependencies and local minima, Struct. Optim. 16 (1998) 68–75.
[21] G. Strang, Introduction to Applied Mathematics, Wellesley-Cambridge Press, Cambridge, 1986.
[22] M. Zamir, The Physics of Pulsatile Flow, Springer-Verlag, New York, 2000.